Indian Journal of Chemistry
Vol. 59A, May 2020, pp. 589-597

Synthesis and characterization of novel chelation-free Zn(II)-azole complexes: Evaluation of antibacterial, antioxidant and DNA binding activity

Sondavid K Nandanwar[a], Shweta B Borkar[b], Bryan Nathanael Wijaya[c], Enkhnaran Bayarra[c], Lei Lottice Anne Piad[c], QiuLi Jin[c], Celine Sheila Tiara[c], Hak Jun Kim[b]* & Naresh H. Tarte[c]*

[a]Department of Marine Convergence Design, Pukyong National University, Busan 48513, Republic of Korea
[b]Department of Chemistry, Pukyong National University, Busan 48513, Republic of Korea
[c]Department of Chemistry and Biology, KSA of KAIST, Busan, Republic of Korea
Email: afpibp@gmail.com

Received 26 July 2019; revised and accepted 20 April 2020

Here, we synthesized novel chelation-free Zn(II)-complexes (**1**-**3**) $[ZnCl_2L_2]$ of monodentate ligands with L = 2-isopropylimidazole (**L1**), 2-methylbenzimidazole (**L2**), and 2-methylbenzoxazole (**L3**) and evaluated their antibacterial, antioxidant and DNA binding activities. The chelation-free properties of these coordination complexes were confirmed by UV-visible spectroscopy, ^{1}H NMR spectroscopy, single X-ray crystallography and elemental analysis. Complexes **1**-**3** exhibited substantial antibacterial activity against all antibiotic susceptible bacteria within a concentration range of 100-200 µg/ml while free ligands **L1** and **L2** exhibited weak antibacterial activity considerably concentration above 200 µg/ml. Also, both complexes **2** and **3** were twice more active against methicillin-resistant *Staphylococcus aureus* (*MRSA)* than complex **1**. Furthermore, we found that complexes **1**-**3** showed DNA binding activity with *E. coli* plasmid DNA and calf thymus DNA, which may be a plausible mechanism for their antibacterial activity. We also investigated the antioxidant activity of complexes **1**-**3** and found that complex **2** exhibited potential antioxidant activity compared to complexes **1** and **3**. All these results suggest that the chelation-free Zn(II)-complexes can be the future candidates for more advance biological studies.

Keywords: Zn(II) complex, 2-isopropylimidazole, 2-methylbenzimidazole, 2-methylbenzoxazole, DNA binding

The continued development of antibiotic-resistant bacteria, as well as a shortage of new antibiotics in the pharmaceutical pipeline, is one of the serious threats to human health in the 21st century[1]. Recently, methicillin-resistant *Staphylococcus aureus* (*MRSA*)[2], an antibiotic-resistant bacteria, gives a challenge for the development of efficient antibacterial agents. *MRSA* can cause serious health problems like skin and soft tissue infections, necrotizing pneumonia, and death[3]. In addition to most beta-lactams antibiotics such as cloxacillin, *MRSA* also developed a resistance to erythromycin, clindamycin, aminoglycosides, fluoroquinolones, rifampicin, and cotrimoxazole[4]. These situations have revealed a substantial medical need to develop new antibiotics with minimal cross-resistance.

The monodentate azole derivatives are present in important biological compounds such as deoxyribonucleic acid, hemoglobin, histidine, Vitamin B12, and histamine[5]. Also, the azole nucleus is a crucial building block in fungicidal drug discovery such as ketoconazole, itraconazole, and fluconazole[6]. Most of the research showed that imidazole derivatives have several medicinal properties, such as antibacterial, anti-inflammatory and analgesic, antidepressant, antitubercular, anticancer, antileishmanial, and antiviral[7]. Lately, imidazole and imidazolium derivatives have been the subject of a thorough study of the antibacterial activity for their potential as promising therapeutic agents[8,9]. Moreover, the coordination of azole with metal ions enhances the biological activity of azoles, which is a consequence of the formation of metal complexes that assist the transport of azole into cells[10,11].

Zn(II) ion is one of the most commonly used antibacterial metal ion and is known to have less cytotoxicity towards mammalian cells[12]. Antibacterial activity of Zn(II) ions is similar to commercially used antibacterial metal ions such as Ag(I) and Cu(II) ions[13]. For many years Zn(II) ions have been added into many dental materials such as mouth rinses and toothpaste due to the ability of Zn(II) ion to inhibit the growth of *albicans* an oral cariogenic bacterium such

as *Streptococcus mutans, Actinomyces viscosus, Lactobacillus casei, Staphylococcus aureus* and *Candidaalbicans*[14,15].

Many chelated Zn(II)-azole complexes have been reported for their antibacterial activity against antibiotic-resistant bacteria such as *MRSA*[16,17]. However, no studies have been reported for the antibacterial activity of chelation-free Zn(II)-azole complexes. The carboxypeptidase-A that hydrolyzes the first peptide or amide bond of proteins is a nice example of chelation-free Zn(II)-histidine complex, which also reveals the bio-compatibility of such chelation-free Zn(II)-azole complexes[18]. Due to the bio-compatibility of Zn(II)-azole moieties, synthetic Zn(II)-azole complexes can easily be absorbed in the human body without any harmful effects[19].

The plausible mechanism of action of coordination complexes for antibacterial activity may be the inhibition of translation or transcription or both processes cause by binding of coordination complexes to DNA[20]. Thus, DNA binding assay of synthesized Zn(II)-complexes was performed against plasmid DNA (pDNA) and calf thymus DNA (CT-DNA). Additionally, the antioxidant activity of synthesized Zn(II)-complexes was performed as most of the Zn(II)-complexes show good antioxidant activities[21]. All these findings promote us to design and synthesize simple, cost-effective, and chelation-free azole complexes of Zn(II) metal ion and to compare their antibacterial activity with chelated Zn(II)-complexes.

Materials and Methods

All chemicals used in this research were purchased from Sigma-Aldrich and used without further purification, those include metal precursor Zn(II) chloride, ligands such as 2-isopropylimidazole, 2-methyl benzimidazole and 2-methyl-benzoxazole, and the experimental solvents dichloromethane (DCM), acetonitrile, diethyl ether, n-hexane, methanol, dimethyl sulfoxide (DMSO) and dimethylformamide.

Experimental Section

Synthesis of dichlorobis(2-isopropylimidazole)Zinc(II) complex(1)

$ZnCl_2$ (5.0 mmol) and 2-isopropylimidazole (10 mmol) were added into two separate clean and dry 100 mL Erlenmeyer flask. Above solids were dissolved with stirring in approximately 20 mL of DCM solvent at room temperature. After complete dissolution, the 2-isopropylimidazole solution was added dropwise into the $ZnCl_2$ suspension. The outcome was stirred for 15 min at room temperature until most of the ligands reacted with $ZnCl_2$ to give white crystals (Scheme 1). White crystals were filtered using a glass funnel-filter setup. The solvent was removed over a rotary evaporator and kept for drying. Dried crystals were washed three times with hexane, filtered, and recrystallized with acetonitrile at room temperature. Then, the crystals were characterized by UV-visible analysis, ^{1}H NMR, and single-X-ray analysis for molecular structure determination. Yield: 72%. Anal. Calcd. for $C_{12}H_{20}N_4Cl_2Zn$ (356.61); C, 40.42; H, 5.65; N, 15.71; Cl, 19.88; Zn, 18.34. Found: C, 40.63; H, 5.44; N, 15.82; Cl, 19.76; Zn, 18.56%.^{1}H NMR (**1**) δ 1.24 (6H, d, J = 6.7 Hz), 3.01 (1H, sept, J= 6.7 Hz), 7.16 (1H, d, J= 3.3 Hz), 7.24 (1H, d, J= 3.3 Hz). UV-visible (DMSO) λ_{max}, nm (log ε, L mol^{-1} cm^{-1}): 287 (2.53).

Synthesis of dichlorobis(2-methylbenzimidazole)zinc(II) complex (2) and dichlorobis(2-methylbenzoxazole)zinc(II) complex (3)

A similar procedure was followed, as above, for the synthesis complexes **2** and **3** (Scheme 1).

Complex 2: Yield: 85%. Anal. Calcd. For $C_{32}H_3Cl_2N_8Zn$ (664.94); C, 57.8; H, 4.85; N, 16.85; Cl, 10.66; Zn, 9.83. Found C, 57.56; H, 4.68; N, 16.58; Cl, 10.48; Zn, 9.62%. ^{1}H NMR (**2**): 2.06 (3H, s), 7.20–7.15 (4H, ddd), 7.63 (1H, s). UV-visible (DMSO) λ_{max}, nm (log ε, L mol^{-1} cm^{-1}): 288 (2.49).

Complex 3: Yield: 64%. Anal. Calcd. For $C_{16}H_{14}C_{l2}N_2O_2Zn$ (402.59); C, 47.73; H, 3.5; N, 6.96; O, 7.95; Cl, 17.61; Zn, 16.24. Found C, 47.83; H, 7.72; N, 6.78; O, 9.68; Cl, 17.55; Zn, 16.29%. ^{1}H NMR (**3**): 2.07–2.04 (3H, s), 7.58–7.42 (2H, 7.32(ddd, J = 8.0, 7.8, 1.6 Hz), 7.37(ddd, J = 8.1, 7.8, 1.8 Hz)), 7.73–7.68 (1H, ddd, J = 8.1, 1.6, 0.5 Hz), 8.23–8.15 (1H, ddd, J = 8.0, 1.8, 0.5 Hz). UV-visible (DMSO) λ_{max}, nm (log ε, L mol^{-1} cm^{-1}): 289 (2.71).

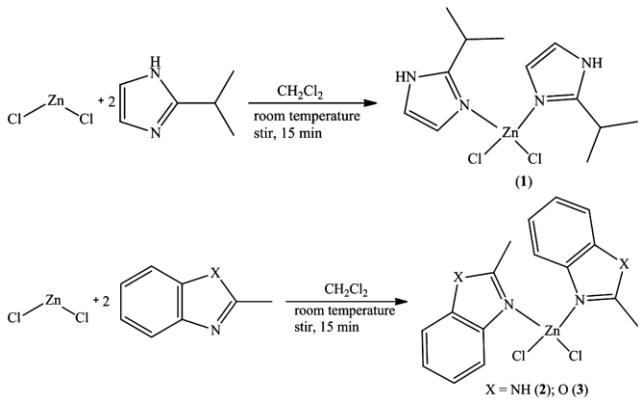

Scheme 1 — Synthesis of Zn(II)-complex (**1-3**).

X-ray structural determination

The single X-ray structure analysis data were collected using a Bruker SMART Apex II X-ray diffractometer, and the structure, solution, and refinement was performed by using the SHELXS program.

Antibacterial assay

Minimum inhibitory concentration is the ending drug concentration that completely inhibits the visible growth of the microorganism in the micro dilution wells. The antibacterial activity of complexes **1-3**, ligands **L1** and **L2**, and streptomycin (positive control) were evaluated by the minimal inhibitory concentrations (MIC) assay. The test compounds were diluted with a twofold serial dilution method under standard conditions[22]. Antibacterial activity was performed against Gram-positive bacteria methicillin-resistant *Staphylococcus aureus* (*MRSA*), *Staphylococcus aureus*, *Bacillus subtilis*, and *Enterococcus faecalis*) and Gram-negative bacteria (*Escherichia coli*, *Klebsiella pneumonia*, and *Salmonella typhimurium*). A single colony of each bacterium was inoculated in 3 mL Luria broth and incubated for 18 h at 37 ℃. Complexes **1-3**, ligands **L1** and **L2**, and streptomycin were dissolved in DMSO. The obtained solution was diluted with sterilize distilled water to give a final concentration of the test in 1% DMSO. Each well was dispensed with 100 µL aliquots of this solution and 100 µL of bacteria inoculums into micro dilution sterileplates (SPL Life Sciences). The final test concentration of bacteria was approximately 2×10^5 CFU mL^{-1}. The final concentration of complexes **1-3**, ligands **L1** and **L2**, and streptomycin were ranged from 1.562 to 200 µg/mL all in twofold dilution steps. Each plate also contained one DMSO control (1% DMSO + bacteria), eight untreated negative controls (1% DMSO + complexes or ligands), and water control (dH_2O + bacteria) to check the effect of 1% DMSO on bacterial growth. These plates were incubated at 37 °C for 18 h. The optical density (OD) of the plates was recorded using a VersaMax Microplate Reader at 650 nm. The minimum inhibitory concentration (MIC) of the complexes **1-3**, and ligands **L1** and **L2** were calculated by subtracting OD of negative control from OD of the sample.

DNA mobility shift assays of plasmid DNA

Plasmid DNA was isolated from 5 ml (OD = 1) transformed *E. coli* PET25b by using the DNA spin Plasmid DNA purification kit (INTRON Biotechnology). The concentration of purified DNA was approximately 40 μg/ 50 μL (according to the information in the catalogue).16 μg (20 μL) of pDNA was incubated at 25 C with 1 mM of the zinc complexes **1-3**. The loading buffer, consisting of 0.25% bromophenol blue, 0.25% xylene cyanol FF, and 30% (v/v) glycerol in water, was added after 60 min to stop the reaction. The resulting mixture of pDNA and complexes were separated by electrophoresis on agarose gels (0.8% w/v), which contained 1 μg/mL ethidium bromide (EB) in 22.25 mM Tris, pH 8, 22.25 mM Boric acid, 0.5 mM EDTA, at low voltage. DNA mobility shift assays were performed in a horizontal gel apparatus (Mupid-2plus Submarine electrophoresis system) for about 2.5 h. The gels were visualized in the presence of UV light.

DNA mobility shift assays of calf thymus DNA

0.08 mM CT-DNA was incubated at 25 °C with 1 mM of zinc complexes **1-3**. At 25 °C, the reaction was terminated after 30 min by the addition of loading buffer consisting of 0.25% bromophenol blue, 0.25% xylene cyanol FF, and 30% (v/v) glycerol in water. The resulting mixture of pDNA and complexes were separated by electrophoresis on agarose gels (1% w/v), which contained 1 μg/mL ethidium bromide (EB) in 22.25 mM Tris, pH 8, 22.25 mM Boric acid, 0.5 mM EDTA, at low voltage. DNA mobility shift assays were performed in a horizontal gel apparatus (Mupid-2plus Submarine electrophoresis system) for about 1 h. The gels were visualized in the presence of UV light.

DPPH radical scavenging assay

DPPH radical scavenging assay was performed with some modification as reported in the literature[23]. We prepared the solution of DPPH in methanol having absorbance of 0.416 at the wavelength of 517 nm. The solutions of different concentrations (25 µg/ml to 400 µg/ml) of complexes **1-3** and rutin had been prepared in N,N-Dimethylformamide, and used for the assay. 1 ml solution of complexes **1-3** and rutin was mixed with 1ml of DPPH solution and incubated in dark for at least 5 h. The absorbance of 1 mL solution of all incubated mixtures was measured at 517 nm after 5 h. DPPH radical scavenging activity was calculated for the different concentrations of complexes using the formula as given below.

$$Percent\ inhibition\ of\ DPPH\ radical = [(A_{br} - A_{ar})/A_{br}] \times 100 \quad \ldots(1)$$

Where, A_{br} is the absorbance before reaction and A_{ar} is the absorbance after the reaction.

Results and Discussion

A series of chelation-free Zn(II)-complexes **1-3** of formula $[ZnCl_2L_2]$ (L= 2-isopropylimidazole (**L1**), 2-methylbenzimidazole (**L2**), and 2-methylbenzoxazole (**L3**)) were synthesized with a typical synthesis procedure as reported earlier by us. Complexes **1-3** were characterized by UV-visible spectroscopy, ^{1}H NMR spectroscopy, single X-ray crystallography, and elemental analysis. The remarkable solubility of complexes **1-3** in the mixture of DMSO-water is a critical first step for possible applications of these complexes in biological systems.

Synthesis of complexes **1-3** was a simple, single-step, and cheap as these reactions were completed in one step within 15 min at room temperature compared to the synthesis of Schiff base and chelated azole Zn(II)-complexes which demand the multi-step synthesis of ligands at high temperature[24,25]. Similarly, the ligands used in complexes **1-3** are commercially available monodentate ligands compared to multi-step synthesized Schiff base ligands used in previous studies[26,27].

Molecular structures of Zn(II)-complexes 1-3

The single X-ray crystal structures of complexes **1-3** are shown in Figs. 1-3, respectively. The crystallographic data and refinement parameters of complexes **1-3** are summarized in Table 1. The coordination geometry around the Zn(II)-complexes **1-3** is distorted tetrahedral similar to analogous Co(II)-complexes previously reported Tarte *et al.*[28]. Table 2 lists the pertinent bond distances and angles of complexes **1-3**. Table 3 lists the hydrogen bonding in complex **1** and **2**. The crystal structures of complexes **1-3** are orthorhombic, monoclinic, and triclinic, respectively. Complex **1** shows inter-molecular hydrogen bonding between amine hydrogen of one of the 2-isopropylimidazole of the first complex and with chlorine atom of another complex N(2)-H(2A)...Cl(1). The crystal structure of complex **1** has extra stability in solid-state because of hydrogen bonding. Complex **2** shows three inter-molecular H-bonding, one of which is between amine hydrogen of one of benzimidazole of the first complex molecule and nitrogen atom of neighboring benzimidazole ligand N(2)-H(2A)...N(5) and vice versa. The second H-bonding is between the amine hydrogen of benzimidazole ligand and one of the

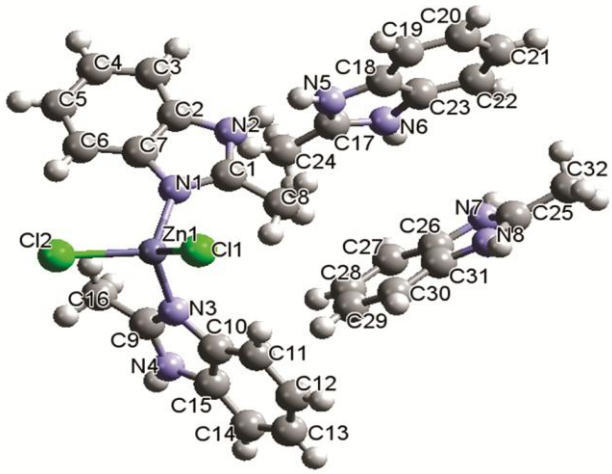

Fig. 2 — Single X-ray crystal structure of dichlorobis(2-methylbenzimidazole)Zn(II) complex (**2**).

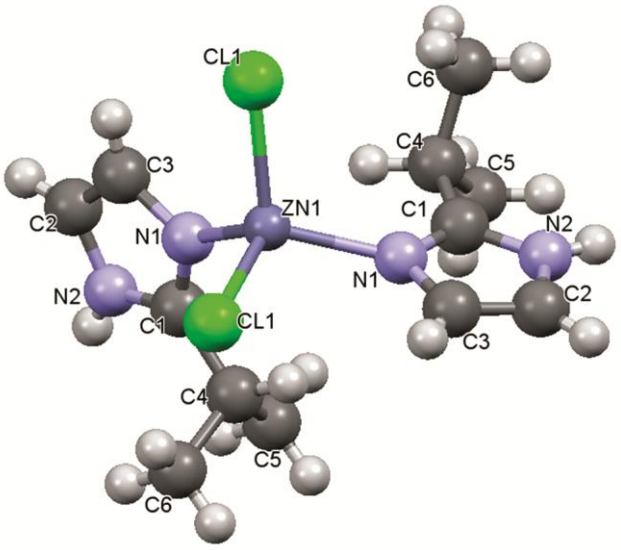

Fig. 1 — Single X-ray crystal structure of dichlorobis(2-isopropylimidazole)Zn(II)complex (**1**).

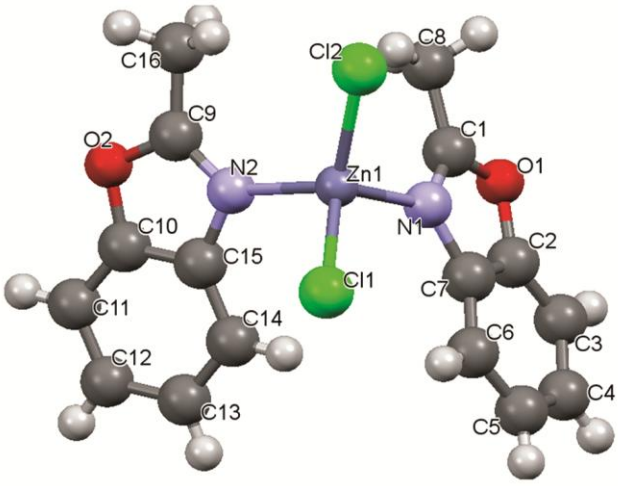

Fig. 3 — Single X-ray crystal structure of dichlorobis(2-methylbenzoxazole)Zn(II) complex (**3**).

Table — 1 Crystallographic data and structure refinement for complexes **1**–**3**

Complexes	**1**	**2**	**3**
Empirical formula	$C_6 H_{10} Cl N_2 Zn_{0.50}$	$C_{32} H_{32} Cl_2 N_8 Zn$	$C_{16} H_{14} Cl_2 N_2 O_2 Zn$
Formula weight	178.29	664.93	402.56
Temperature	298(1) K	296(2) K	296(1) K
Wavelength	0.71073 Å	0.71073 Å	0.71073 Å
Crystal system	Orthorhombic	Monoclinic	Triclinic
Space group	Pbcn	P2(1)/n	P-1
Unit cell dimension	a = 11.1941(2) Å, α = 90° b = 11.3578(2) Å, β = 90° c = 13.0719(3) Å, γ = 90°.	a = 9.6964(2) Å, α = 90°. b = 22.0789(4) Å, β = 97.5710(10) ° c = 15.4249(3) Å, γ = 90°	a = 6.6357(2) Å, α = 85.5930(10) ° b = 10.3514(2) Å, β = 79.4650(10) ° c = 12.9200(3) Å, γ = 73.9100(10) °
Volume	1661.97(6) $Å^3$	3273.46(11) $Å^3$	838.00(4) $Å^3$
Z	8	4	2
Density (calculated)	1.425 mg/m^3	1.349 mg/m^3	1.595 mg/m^3
Absorption coefficient	1.792 mm^{-1}	0.948 mm^{-1}	1.793 mm^{-1}
F(000)	736	1376	408
Crystal size	0.22 x 0.16 x 0.12 mm^3	0.25 x 0.20 x 0.10 mm^3	0.38 x 0.38 x 0.20 mm^3
Theta range for data collection	2.99 to 30.12°	1.84 to 28.28°	1.60 to 28.29°
Index ranges	0<=h<=15, 0<=k<=16, 0<=l<=18	-12<=h<=12, 0<=k<=29, 0<=l<=20	-8<=h<=8, -13<=k<=13, 0<=l<=17
Reflections collected	2423	8094	4132
Independent reflections	2423 [R(int) = 0.0000]	8094 [R(int) = 0.0000]	4132 [R(int) = 0.0000]
Completeness to theta = 28.28°	98.8 %	99.8 %	99.3 %
Absorption correction	Multi-scan	Multi-scan	Multi-scan
Max. and min. transmission	0.8137 and 0.6939	0.9111 and 0.7974	0.7156 and 0.5490
Refinement method	Full-matrix least-squares on F^2	Full-matrix least-squares on F^2	Full-matrix least-squares on F^2
Data / restraints / parameters	2423 / 0 / 87	8094 / 0 / 388	4132 / 0 / 211
Goodness-of-fit on F^2	1.042	1.034	1.081
Final R indices [I>2sigma(I)]	R1 = 0.0365, wR2 = 0.0970	R1 = 0.0463, wR2 = 0.1207	R1 = 0.0283, wR2 = 0.0754
R indices (all data)	R1 = 0.0567, wR2 = 0.1074	R1 = 0.0694, wR2 = 0.1351	R1 = 0.0314, wR2 = 0.0794
Largest diff. peak and hole	0.834 and -0.249 e.Å $^{-3}$	0.740 and -0.293 e.Å $^{-3}$	0.368 and -0.404 e.$Å^{-3}$

Table —2 Comparison of selected bond lengths (A˚) and angles (°) for complexes **1**–**3**

Complex **1**	Complex **2**	Complex **3**
Zn(1)-N(1) - 1.9980(16)	Zn(1)-N(1) - 2.0176(18)	Zn(1)-N(2) - 2.0642(15)
Zn(1)-N(1)#1 - 1.9980(16)	Zn(1)-N(3) - 2.0283(18)	Zn(1)-N(1) - 2.0646(16)
Zn(1)-Cl(1) - 2.2598(5)	Zn(1)-Cl(1) - 2.2480(7)	Zn(1)-Cl(2) - 2.2147(5)
Zn(1)-Cl(1)#1 - 2.2599(5)	Zn(1)-Cl(2) - 2.2721(7)	Zn(1)-Cl(1) - 2.2282(5)
N(1)-Zn(1)-N(1)#1 - 115.91(9)	N(1)-Zn(1)-N(3) - 104.95(8)	N(2)-Zn(1)-N(1) - 98.61(6)
N(1)-Zn(1)-Cl(1) - 109.50(5)	N(1)-Zn(1)-Cl(1) - 109.47(6)	N(2)-Zn(1)-Cl(2) - 115.56(5)
N(1)#1-Zn(1)-Cl(1) - 106.07(4)	N(3)-Zn(1)-Cl(1) - 113.79(5)	N(1)-Zn(1)-Cl(2) - 109.93(5)
N(1)-Zn(1)-Cl(1)#1 - 106.07(4)	N(1)-Zn(1)-Cl(2) - 112.56(6)	N(2)-Zn(1)-Cl(1) - 105.81(4)
N(1)#1-Zn(1)-Cl(1)#1 - 109.50(5)	N(3)-Zn(1)-Cl(2) - 107.77(6)	N(1)-Zn(1)-Cl(1) - 111.69(5)
Cl(1)-Zn(1)-Cl(1)#1 - 109.74(3)	Cl(1)-Zn(1)-Cl(2) - 108.35(3)	Cl(2)-Zn(1)-Cl(1) - 114.19(2)

chlorine atoms of first complex N(6)-H(6A)...Cl(1), while third H-bonding is between the iminium hydrogen of the benzimidazole ligand and chlorine atom of first complex [N(7)-H(7A)...Cl(2)#2]. In complex **2**, each complex molecule is bonded with two neighboring benzimidazole ligands via inter-molecular H-bonding, giving high stability to the crystal structure in solid-state. Complex **3** does not show any hydrogen bond in the crystal due to the absence of an amine N-H group in it.

Furthermore, the N-Zn-N bond angle in complexes **1**, **2** and **3** are 115.91º, 104.95º, and 98.61º, respectively. The Cl-Zn-Cl bond angle of complexes **1**, **2**, and **3** are 109.74º, 108.35º, and 114.19º, respectively. The reason for the higher N-Zn-N bond angle in complex **1** compared to complexes **2** and **3** may be the steric hindrance between two imidazole ligands due to the repulsion between two bulkier isopropyl substituents. The moderate N-Zn-N bond angle in complex **2** compared to complex **1** and **3** may be due to intermolecular hydrogen bonding with benzimidazole ligands. The bond angle between Cl-Zn-Cl in complexes **1** and **2** is less compared to complex **3**, which may result from steric hindrance

Table — 3 Hydrogen bond lengths (Å) and angles (°) for complexes **1** and **2**

Complex	D-H...A	d(D-H)	d(H...A)	d(D...A)	<(DHA)
1[a]	N(2)-H(2A)...Cl(1)#2	0.86	2.51	3.357(19)	166.6
2[b]	N(2)-H(2A)...N(5)	0.86	2.01	2.826(3)	157.7
	N(4)-H(4A)...N(8)#1	0.86	1.98	2.810(3)	161.5
	N(6)-H(6A)...Cl(1)#2	0.86	2.55	3.366(2)	159.2
	N(7)-H(7A)...Cl(2)#2	0.86	2.40	3.251(2)	170.3

Symmetry transformations used to generate equivalent atoms:
a = #1 -x, y, -z+1/2 #2 -x+1/2, y-1/2, z
b = #1 x-1, y, z #2 -x+1/2, y+1/2, -z+3/2

Table — 4 MIC values of complexes **1**–**3** and ligands **L1** and **L2** in µg/mL

	Bacteria	**1**	**2**	**3**	**L1**	**L2**	**Streptomycin**
Gram positive	*MRSA*	100	50	50	> 200	> 200	> 200
	S. aureus	100	100	200	> 200	> 200	1.526
	B. subtilis	200	100	100	> 200	> 200	3.052
	E. faecalis	200	100	200	> 200	> 200	3.052
Gram negative	*E. coli*	100	100	100	> 200	>200	1.526
	S. typhimurium	100	100	200	> 200	> 200	6.104
	K. pneumoniae	100	200	200	> 200	> 200	3.052

between their respective ligands (2-isopropylimidazole and 2-methylbenzimidazole), while complex **3** does not have a steric hindrance between 2-methylbenzoxazole. Both Zn-N bond lengths in complex **1** [1.9980 A˚] are symmetric, while that of complexes **2** [2.0176(18) A˚ and 2.0283(18) A˚], and **3** [2.0642(15) A˚ and 2.0646(16) A˚] are more asymmetric. The density of the complexes **1**, **2** and **3** are 1.425 mg/m^3, 1.349 mg/m^3 and 1.595 mg/m^3, respectively. The space group of the complexes**1**, **2** and **3** are Pbcn, P2(1)/n, and P-1, respectively. These results indicate that complexes **1**, **2** and **3** have different nucleation mechanisms.

Antibacterial activity

The in vitro antibacterial activity of complexes **1-3** and ligands **L1** and **L2** were examined against Gram-positive strains (methicillin-resistant *Staphylococcus aureus* (*MRSA*), *Staphylococcus aureus*, *Bacillus subtilis*, and *Enterococcus faecalis*) and Gram-negative strains (*Escherichia coli*, *Salmonella typhimurium*, and *Klebsiella pneumoniae*) with streptomycin as a positive control. Their MIC values were ranged between 1.56 to 200 µg/mL using a two-fold serial dilution method. Positive control displayed significant antibacterial activity against all strains of tested bacteria except *MRSA*, whereas negative control and solvent control displayed no observable antibacterial activity against any of the test organisms, as shown in Table 4. Complexes **1** and **2** were twice more potent against *S. aureus*, and *S. typhimurium* with a MIC value of 100 µg/mL compared to complex **3** with MIC value of 200 µg/mL. Complexes **2** and **3** were twice more potent against *B. subtilis* with a MIC value of 100 µg/mL compared to complex **1** with a MIC value of 200 µg/mL. Complexes **1** and **3** were twice more potent against *E. faecalis* with a MIC value of 100 µg/mL compared to complex **2** with a MIC value of 200 µg/mL. Complex **1** was twice more potent against *K. pneumoniae* with a MIC value of 100 µg/mL compared to complexes **2** and **3** with a MIC value of 200 µg/mL. Complexes **1-3** displayed similar antibacterial activity against *E. coli* with a MIC value of 100 µg/mL. Complexes **2** and **3** displayed excellent antibacterial activity against *MRSA* with a MIC value of 50 µg/mL, which was twice more compared to complex **1** with a MIC value of 100 µg/mL.

All these results showed that complexes **1-3** displayed non-selective antibacterial activity against tested bacterial strain. There was a substantial increase in antibacterial activity of free ligands **L1** and **L2** against tested bacterial strain on coordination with Zn(II) ion[29]. Complexes **1-3** showed very high antibacterial activity compared to reported zinc complex and other metal complexes against antibiotic susceptible bacteria[30,31]. Complexes **1-3** displayed more antibacterial activity compare to chelated Zn(II)-benzimidazole complex against *MRSA*[32]. Complexes **1-3** were found to be 2.5 to 5-foldmore activity against *MRSA* compared to macrocyclic Zn(II) Schiff base complex[26]. Zn(II)-complexes of Schiff base ligands did not display antibacterial activity against *MRSA*[27,33].

Delocalization of π-electrons over the whole complex ring may increase the lipophilicity of the complex compared with the free ligands, which enhance the penetration of the complex into the lipid membranes of the microorganisms[34]. Furthermore, the plausible mechanism of action for antibacterial activity of complexes **1-3** may be the inhibition of translation or transcription or both processes caused by binding of complexes **1-3** to DNA[20,35].

DNA mobility shift assay

DNA multiplication is one of the pivotal events during cell division, and it is one of the key targets for antibacterial activity[20]. It is well-known that most of the metal complexes form strong interaction with DNA[36]. Thus, DNA mobility shift assays were carried out to investigate the ability of complexes **1-3** to interact with pDNA and CT-DNA.

DNA mobility shift assays of plasmid DNA

An initial amount of pDNA was incubated with complexes **1-3 (**1mM**)**. In DNA mobility shift assays, untreated supercoiled pDNA shows a relatively fast migration compared to treated supercoiled pDNA. However, if binding occurs between complexes and pDNA, the supercoil pDNA will relax to generate a slower-moving relax form[37].The breakdown of a single strand of pDNA may lead to the occurrence of a DNA smear upon gel electrophoresis[38].

Fig. 4 shows the gel electrophoretic mobility shift of pDNA before (Lane 1) and after (Lane 2-4) incubation with complexes **1-3**. pDNA is the mixture of the supercoiled form (upper band) and circular form (lower band). Complexes **1** and **2** led to the formation of a DNA smear, indicating extensive breaking of DNA strand, resulting in DNA degradation. Complex **3** interacts with pDNA which leads to the formation of the wide intense band in the upper band.

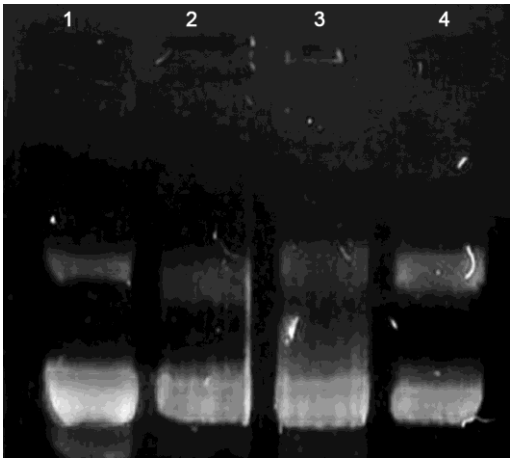

Fig. 4 — Agarose gel electrophoresis pattern of pDNA in the presence of complexes **1**–**3**. Lane 1, DNA control; lane 2, DNA + **1** (1 mM); lane 3, DNA + **2** (1mM); lane 4, DNA + **3** (1 mM).

DNA mobility shift assays of calf thymus DNA

An initial amount of CT-DNA was incubated 1mM concentrations of the complexes **1-3**. When CT-DNA was subject to the DNA mobility shift assays, relatively fast migration was observed for the untreated CT-DNA. However, if binding occurs between complexes and CT-DNA, the latter get relaxed to generate a slower-moving relax form. The precession of the electrophoretic mobility is associated with the degradation of the CT-DNA[35].

Fig. 5 shows the gel electrophoretic mobility shift of CT-DNA before (lane 1) and after (lane 2-4) incubation with complexes **1-3**. Complexes **1-3** shifted the mobility of CT-DNA substantially, which indicated the strong interaction of complexes **1-3** with CT-DNA. Complex **3** showed strong interaction with CT-DNA as compared to complexes **1** and **2**. DNA mobility shift assays revealed that complexes **1** and **2** lead to the cleavage of pDNA and shift the mobility of CT-DNA. These results indicate that bacterial DNA cleavage is a plausible mechanism of action for the antibacterial activity of complexes **1** and **2**. Complex **3** does not cleave pDNA but form strong interaction with pDNA and CT-DNA. Complex **3** may have different mechanisms of action compared to complexes **1** and **2**.

Antioxidant activity

The aim of this experiment is to determine the radical scavenging activity of complexes **1-3** by the DPPH method in comparison to rutin[39].

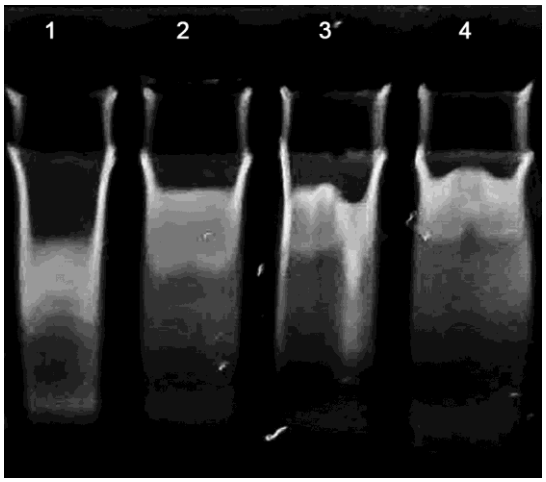

Fig. 5 — Agarose gel electrophoresis pattern of CTDNA in the presence of the synthesized zinc complexes **1-3**. Lane 1, CTDNA control; lane 2, DNA + **1** (1 mM); lane 3, DNA + **2** (1 mM); lane 4, DNA + **3** (1 mM).

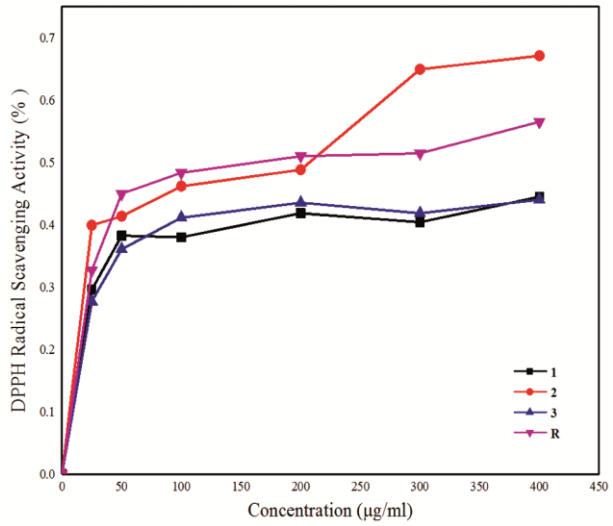

Fig. 6 — Antioxidant activity of complexes **1-3**.

1,1-Diphenyl-2-picrylhydrazyl (DPPH) radical scavenging activity

DPPH is a stable free radical having strong purple color in methanol. It easily reacts with hydrogen atom donor moiety and electron donor moiety, which leads to a decrease in color intensity of DPPH to give a final reduced product with yellow color. To determine the antioxidant activity of desired compounds, this is the simple and best technique. Complex **2** showed higher radical scavenging activity compared to complexes 1 and 3, and rutin. The decreasing order of radical scavenging activity of complexes **1-3** and rutin is as follows: **2** > **R** > **3** > **1** (Fig. 6). The plausible mechanism of action for antioxidant activity of complexes **1-3** may be the abstraction of hydrogen free radical of amine or methyl group[40]. Under the influence of resonance and inductive effects, abstraction of hydrogen atom may occur easily. The molecules get stabilized due to resonance and inductive effects, which may facilitate the release of hydrogen atom[41].

Conclusions

Three novel chelation-free Zn(II)-complexes (**1-3**) $[ZnCl_2L_2]$ were synthesized and structurally characterized. Based on UV-visible spectroscopy, ^1H NMR spectroscopy, single X-ray crystallography, and elemental analysis, the chelation-free property of pseudo-tetrahedral Zn(II)-complexes (**1-3**) were confirmed. Complexes **1-3** exhibited the nonselective antibacterial activity against all tested bacterial strains. Complexes **2** and **3** exhibited the highest antibacterial activity against *MRSA* with a MIC value of 50 µg/mL. pDNA mobility shift assay suggests that complexes **1** and **2** lead to the degradation of pDNA, while complex **3** efficiently shifts the mobility of pDNA. CT-DNA mobility shift assays suggest all the complexes bind to CT-DNA. Additionally, Zn(II)-complexes (**1-3**) also displayed good antioxidant activity. Therefore, the information obtained from the present work suggests that the chelation-free Zn(II)-complexes (**1-3**) can be the future candidates for more advance biological studies.

Acknowledgement

This work was supported by the Korean Science Academy of KAIST and Basic Science Research Program through the National Research Foundation of Korea with funds from the Ministry of Science and ICT (NRF-2015R1A2A2A01005609). Mr. Sondavid K Nandanwar is thankful to the Department of Chemistry and Biology KSA of KAIST for this cooperative research.

References

1 Nandanwar S K & Kim H J, *Chem Select*, 4 (2019) 1706.
2 Kavanagh K, Müller-Bunz H, Beirne C O, Tacke M, Dada O, Ortin Y, Althani H T, Cassidy J & Zhu X, *Polyhedron*, 149 (2018) 95.
3 Moghnieh R, Alothman A F, Althaqafi A O, Matar M J, Alenazi T H, Farahat F, Corman S L, Solem C T, Raghubir N, Macahilig C & Stephens J M, *J Infect Public* Health, 10 (2017) 849.
4 Thabit A K, Fatani D F, Bamakhrama M S, Barnawi O A, Basudan L O & Alhejaili S F, Int *J Infect Dis*, 81 (2019) 128.
5 Fodor C, Stumphauser T, Thomann R, Thomann Y & Iván B, *Polym Chem*, 7 (2016) 5375.
6 Leonardi D, Alvarez V A, Calvo N L, Quiroga A D, Svetaz L A & Lamas M C, *Int J Pharm*, 556 (2018) 181.
7 Kim H S, Jadhav J R, Jung S J & Kwak J H, *Bioorg Med Chem Lett*, 23 (2013) 4315.
8 Wu X, Wang G X, Shen Y, Hu Y & Tu X, Eur *J Med Chem*, 143 (2017) 958.
9 Zheng Z, Xu Q, Guo J, Qin J, Mao H, Wang B & Yan F, *ACS Appl Mater Interfaces*, 8 (2016) 12684.
10 Bello-Vieda N J, Pastrana H F, Garavito M F, Ávila A G, Celis A M, Muñoz-Castro A, Restrepo S & Hurtado J J, *Molecules*, 23 (2018) 1.
11 Bharty M K, Dani R K, Nath P, Bharti A, Singh N K, Prakash O, Singh R K & Butcher R J, *Polyhedron*, 98 (2015) 84.
12 Taylor K M, Solfa F, Jones A T, Wiggins H L, Westwell A D, Hiscox S E & Wymant J M, *Biochem Pharmacol*, 93 (2015) 332.
13 Singha P, Pant J, Hopkins S P, Workman C D & Handa H, *J. Biomed. Mater*. Res. Part A, 107 (2019) 1425.
14 Almoudi M M, Hussein A S, Abu Hassan M I & Zain N M, *Saudi Dent* J, 30 (2018) 283.
15 Yakoob J, Naz S, Awan S, Abbas Z, Jafri W, Hamid S, Jafri F & Usman M W, *Microb Drug Resist*, 20 (2013) 305.
16 Ashraf A, Siddiqui W A, Akbar J, Mustafa G, Krautscheid H, Ullah N, Mirza B, Sher F, Hanif M & Hartinger C G, *Inorg Chim Acta*, 443 (2016) 179.

17 Indoria S, Lobana T S, Sood H, Arora D S, Hundal G & Jasinski J P, *New J Chem*, 40 (2016) 3642.
18 Jeyaharan D, Brackstone C, Schouten J, Davis P & Dixon A M, *ChemBioChem*, 19 (2018) 1898.
19 Vanco J, Sindela Z, Dvorak Z & Travnicek Z, *J Inorg Biochem*, 142 (2015) 92.
20 Butler J A, Li X, Poole R K & Collins J G, *ChemPlusChem*, 83 (2018) 643.
21 Papadopoulos A N, Zoi I, Raptopoulou C P, Kessissoglou D P, Tarushi A, Psycharis V, Kakoulidou C & Psomas G, *J Inorg Biochem*, 170 (2017) 85.
22 Devi J, Yadav M, Kumar D, Naik L S & Jindal D K, *Appl Organomet Chem*, 33 (2019) 1.
23 Ghosh A, Igamberdiev A U & Debnath S C, *Sci Rep*, 8 (2018) 1.
24 Li S, Chen J, Xiang Q, Zhang L & Zhou C, Eur *J Med Chem*, 84 (2014) 677.
25 Vijayakumar V, Rajesh J, Amali I B, Rajagopal G, Gandhi N I & Kesavan M P, *J Mol Struct*, 1183 (2019) 342.
26 Shalini A S S, Amaladasan M, Prasannabalaji N, Revathi J & Muralitharan G, *Arabian J Chem*, 12 (2014) 1176.
27 Mcginley J, Mccann M, Ni K, Tallon T, Kavanagh K, Devereux M, Ma X & Mckee V, *Polyhedron*, 55 (2013) 169.
28 Tarte N H, Woo S I, Cui L, Gong Y D & Hwang Y H, *Organomet Chem*, 693 (2008) 729.
29 Singh K, Kumar Y, Puri P & Sharma C, *Arabian J Chem*, 10 (2017) S978.
30 Mallikarjuna N M, Keshavayya J, Maliyappa M R, Shoukat Ali R A & Venkatesh T, *J Mol Struct*, 1165 (2018) 28.
31 Ejidike I P, *Molecules*, 23 (2018) 1.
32 Poyraz M, Sarı M, Şahin E, Güney A, Demirci F & Demirayak S, *J Coord Chem*, 61 (2008) 3276.
33 Gwaram N S, Ali H M, Saharin S M, Abdulla M A, Lin T K, Ching C L & Ooi C L, *J Appl Pharm Sci*, 2 (2012) 27.
34 Nejad F K, Khosravan M, Ebrahimipour S Y & Baseline F, *Appl Organomet Chem*, 32 (2018) 1.
35 Khosravi F & Mansouri-torshizi H, *J Biomol Struct Dyn*, 1102 (2018) 1.
36 Li S T, Ma Z Y, Liu X, Tian J L & Yan S P, *Appl Organomet Chem*, 31 (2017) 1.
37 Huq F, Yu J Q, Daghriri H & Beale P, *J Inorg Biochem*, 98 (2004) 1261.
38 Li R E, Li Y R, Zhu H & Jia Z, *React Oxyg Species*, (2018) 406.
39 Udilova N, Kozlov A V & Bieberschulte W, *Biochem Pharmacol*, 65 (2003) 59.
40 Al-amiery A, Free Radicals *Antioxid*, 6 (2016) 173.
41 Wu H, Yuan J, Bai Y, Wang H, Pan G & Kong J, *J Photochem Photobiol B*, 116 (2012) 13.